# A STUDY OF VIABILITY AND CHARACTERISTIC OF 3D-PRINTABLE MORTAR WITH YELLOW RIVER SAND

JIAPAN SUN[1] , BINGBING FAN[2] , BIN LI[3] and YIMENG ZHANG[4]
[1,2]*University College London*
[3]*Manchester School of Architecture*
[4]*North China University of Water Resources and Electric Power*
[1]*jiapan.sun.23@ucl.ac.uk, 0009-0005-6319-277X*
[2]*bingbing.fan.23@ucl.ac.uk, 0009-0005-2133-7125*
[3]*bin.li3@stu.mmu.ac.uk, 0009-0002-63051377*
[4]*zhangyimeng@ncwu.edu.cn, 0009-0002-7271-0143*

**Abstract.** This study explores the feasibility of formulating cement-based 3D printing mortar by incorporating Yellow River sand as an aggregate. Through systematic testing of the printing performance of Yellow River sand 3D mortar with varying proportions, preliminary insights into a formulation suitable for 3D printing of Yellow River sand mortar have been elucidated. Concurrently, the investigation employs the prepared desert sand 3D printing mortar with a robotic platform and an autonomously developed storage-extrusion 3D printing tool head to conduct 3D printing experiments for the designed samples. This comprehensive process validates the feasibility of 3D printing utilizing Yellow River sand mortar. Moreover, this research broadens the utilization scenarios of Yellow River sand and introduces an innovative approach and methodology for dredging and silt removal in the Yellow River.

**Keywords.** 3D Mortar Printing, The Yellow River Sand; Printing Performance, Mix-ratio Optimization Design, Printing Validation, SDG 9, SDG 11.

## 1. Introduction

The Yellow River ranked as China's second-longest river and concurrently holding the title of the world's river with the highest sediment load, faces persistent challenges of severe sedimentation and riverbed elevation. These issues have significantly undermined the economic efficiency of the river's development. Consequently, the Yellow River basin has progressively evolved into a region marked by a concentrated population of impoverished individuals. In response to these challenges, China has recently embarked on a strategic initiative to establish the Yellow River Ecological Economic Belt. This development has spurred an increasing body of scholarly research to explore the optimal utilization of Yellow River sediments.

China's Yellow River boasts substantial sediment reserves, particularly in the

*ACCELERATED DESIGN, Proceedings of the 29th International Conference of the Association for Computer-Aided Architectural Design Research in Asia (CAADRIA) 2024*, Volume 3, 161-170. 

more accessible lower reaches, indicating considerable developmental potential. However, intrinsic characteristics such as loose accumulation, a rough surface, fine particle size, and a relatively small fineness modulus render Yellow River sand unsuitable for direct use as a fine aggregate in mortar preparation. Presently, Yellow River sand finds limited application in construction materials, primarily confined to fabricating architectural components such as stone, bricks, and tiles. In contrast, contemporary 3D printing technology in construction predominantly utilizes fine aggregates in cement-based 3D printing materials, necessitating the supplementary use of cementitious materials. The attributes of this material system create the potential for integrating natural ultrafine sands like Yellow River sand into 3D printing mortars. The prospective development of a Yellow River sand-based mortar tailored for 3D printing signifies a novel strategy for leveraging this resource. This innovation holds the potential to address the substantial sedimentation issues in the Yellow River, contribute to the progression of construction technologies in the Yellow River basin, and play a pivotal role in mitigating carbon emissions.

This study is conducted against the backdrop of exploring how to utilize Yellow River sand as aggregate to prepare cement-based 3D printing mortar with favorable performance. By integrating with 3D printing technology, the research investigates the utilization of Yellow River sand in 3D printing mortar to manufacture components with unique shapes. Furthermore, it attempts to explore the construction of flood barriers using this mortar.

## 2. Methods and Material

In pursuit of the objectives outlined in this study, we conducted micro-level examinations of various sands to acquire essential parameters specific to Yellow River sand. Following this, 3D printing mortars were formulated, varying in binder-to-sand mass ratios, and rheological printing tests were executed to determine the optimal proportions.Upon establishing the mortar ratios, we devised 3D printing test experiments and implemented a parameter-based workflow. Subsequently, a tailored storage-extrusion 3D printing tool head was designed and manufactured. The final phase involved utilizing the AR4 six-axis robotic platform to execute the printing of the samples.

### 2.1 MATERIAL

3D printing mortar demands high flowability, setting time, constructability, and extrudability requirements. This implies that the material must exhibit excellent flowability during transportation, possess a rapid setting time, and attain high early strength. It is imperative to ensure that the mortar can withstand the load of subsequent layers during the 3D printing process before hardening, thereby guaranteeing the structure's integrity. Consequently, it is essential to design an appropriate mortar mix to ensure the success of subsequent 3D printing experiments.

#### *2.1.1Raw Materials*

In this study, the raw materials for 3D printing mortar primarily consist of P·O 52.5-grade cement as the binder material, Yellow River sand from the Huayuankou section

in Zhengzhou as the fine aggregate, and external additives including polycarboxylate superplasticizer, dispersible latex powder, high-viscosity cellulose ether, and defoaming agent. Before conducting the proportioning study, performing relevant performance tests on the raw materials is essential. This ensures a comprehensive understanding of the mechanistic aspects of mix design and 3D printing test analyses.

In the initial phase of this study, we conducted an XRF (X-ray Fluorescence) chemical composition analysis to scrutinize the chemical constituents of Yellow River sand. The principal components and their respective proportions are outlined in Table 1.

Table 1. Particle size distribution of Yellow River sand

| | D10 | D25 | D50 | D75 | D100 |
|---|---|---|---|---|---|
| Yellow River sand. μm | 125 | 175 | 257 | 325 | 600 |

Subsequently, a PSD (Particle Size Distribution) analysis was performed to ascertain the particle size distribution of Yellow River sand within the range of 0 to 600 micrometers. The resulting particle size distribution and corresponding proportions are presented in Table 2.

Table 2. Chemical composition of Yellow River sand

| | SiO2 | CaO | LOI | Al2O3 | MgO | K2O | Fe2O3 | Na2O |
|---|---|---|---|---|---|---|---|---|
| Yellow River sand wt.% | 55.84 | 14.40 | 10.14 | 9.57 | 2.54 | 2.32 | 2.45 | 2.08 |

Furthermore, an analysis of the roundness, aspect ratio, and roughness was carried out on commonly used manufactured sand, ordinary river sand, and Yellow River sand within the construction market of the Yellow River basin. This analysis was conducted using SEM (Scanning Electron Microscopy), and the results are depicted in Figure 1. The outcomes suggest that Yellow River sand particles, unlike ordinary river sand, exhibit a closer approximation to a circular shape and a smoother surface. This observation implies that, under identical slump conditions, the 3D printing mortar prepared with Yellow River sand will likely demonstrate improved porosity and compactness compared to that prepared with ordinary river sand.

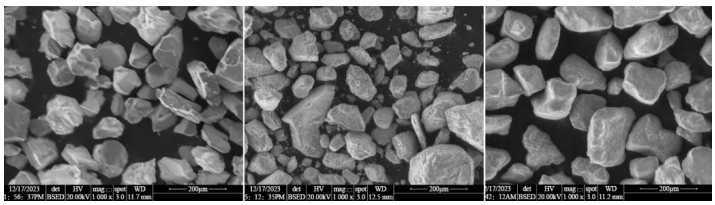

Figure 1. From left to right,manufactured sand,ordinary river sand,and Yellow River sand

The cement utilized in this study is P·O52.5 ordinary Portland silica fume cement. Ordinary Portland silica fume cement is a hydraulic binder comprised of cement clinker, 5%~20% supplementary materials, and gypsum. It exhibits fast hydration

reaction rates, minimal shrinkage during curing, and is less prone to cracking. The technical specifications of this cement are detailed in Table 3.

Table 3. PO52.5 Technical indicators

| CaO (%) | SiO3 (%) | Initial setting time (min) | Final setting time (min) | Specific surface area ($m^2/g$) | Density ($g/cm^3$) |
|---|---|---|---|---|---|
| 64.93 | 3.35 | 157 | 202 | 0.35 | 3.25 |

Although additives constitute a minor proportion of the overall composition of 3D printing mortar raw materials, they can significantly impact the printing performance, including flowability, setting time, constructability, and extrudability. Therefore, judiciously controlling the dosage of additives is particularly crucial.

### *2.1.2Mortar Mix Design*

Based on a review of relevant literature, this study established water-to-cement ratios of 0.44, 0.38, and 0.33 as the mix designs (Huo et al.,2020). 3D printing mortars were then prepared by configuring different binder-to-sand mass ratios. The sample mix designs are detailed in Table 4.

Table 4. The Experimental Proportioning of Yellow River Sand for 3D Printing Mortar Material

| | Water-to-Cement Ratio | Cement | Yellow River sand | Admixture | Defoamer | Fiber |
|---|---|---|---|---|---|---|
| A-1 | 0.44 | 800g | 1200g | 0.8% | 0.1% | 0.1% |
| A-2 | 0.44 | 1100g | 900g | 0.8% | 0.1% | 0.1% |
| B-1 | 0.38 | 800g | 1200g | 0.8% | 0.1% | 0.1% |
| B-2 | 0.38 | 1100g | 900g | 0.8% | 0.1% | 0.1% |
| C-1 | 0.33 | 800g | 1200g | 0.8% | 0.1% | 0.1% |
| C-2 | 0.33 | 1100g | 900g | 0.8% | 0.1% | 0.1% |

Testing sample printing performance primarily involves comparing four aspects: flowability, setting time, constructability, and extrudability. Flowability testing is conducted by the Chinese standard GB/T 2419-2005 to determine the flowability of 3D printing mortar within 80 minutes. Measurements are taken at 20-minute intervals, with the flowability recorded at the 20-minute mark as the initial flowability of the 3D printing mortar. Although additives constitute a minor proportion of the overall composition of 3D printing mortar raw materials, they can significantly impact the printing performance, including flowability, setting time, constructability, and extrudability. Therefore, judiciously controlling the dosage of additives is particularly crucial.

The setting time is determined according to the penetration resistance method

specified in the Chinese standard JGJ/T70-2009 for measuring the open time of 3D printing mortar. A penetration resistance apparatus is employed to measure the penetration resistance values of the 3D printing mortar at 20-minute intervals over a duration of 120 minutes. The result obtained at the 20-minute mark is considered the initial penetration resistance value.

The constructability is evaluated using the mold model to assess the 3D printing mortar's constructability. Specifically, if there is neither visible collapse nor noticeable deformation at a particular height, it indicates good constructability of the mortar at that height. This study determines constructability by printing different samples to the same height and observing their shape retention within 80 minutes. Observations are made every 20 minutes, and the results obtained at the 20-minute mark are considered the initial constructability values (Zhang et al.,2018).

The extrudability is determined using the molding extrusion method. The mortar samples are extruded into elongated strips through a nozzle with a 10mm printing tool head, as illustrated in Figure 2. Extrusion tests are conducted along a 250mm straight line, a 150mm straight line, a 100mm straight line, an L-shaped path, and an S-shaped curve. The extrudability of the mortar samples is assessed by observing the continuity and stability of the extruded strips (Le et al.,2012).

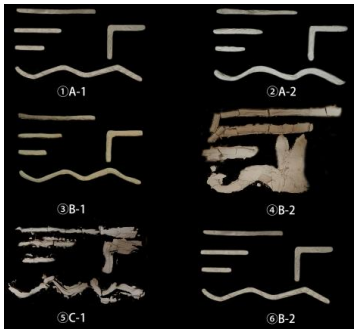


Figure 2. Extrusion testing of mortar samples with different ratios

The results of the printing performance tests for each sample are presented in Table 5 following experimental recordings. Sample B-1 was selected for subsequent 3D printing validation based on the assessment.

Table 5. Evaluation of printability of mortars with different ratios

| | Flowability | Setting time | Constructability | Extrudability | Performance Evaluation |
|---|---|---|---|---|---|
| A-1 | 180mm | Excellent | Excellent | Good | Good |
| A-2 | 220mm | Excellent | Good | Excellent | Good |
| B-1 | 210mm | Excellent | Excellent | Excellent | Excellent |
| B-2 | 250mm | Inoperable | Inoperable | Inoperable | Inoperable |
| C-1 | 170mm | Good | Excellent | Inferior | Inferior |
| C-2 | 220mm | Good | Good | Excellent | Good |

## 2.2 EQUIPMENT

A complete mortar 3D printing system primarily consists of a storage-extrusion system, a robotic system, and a data control system, as illustrated in the workflow depicted in Figure 3. The coordination and design between these systems are essential to achieve the final 3D printing results.

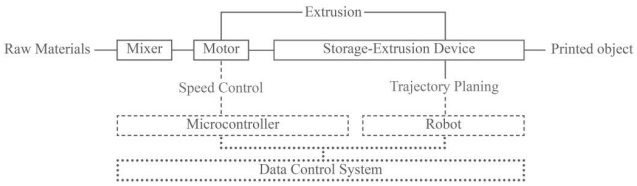


Figure 3. Composition of the mortar 3D printing work system

This study employed the AR4 six-axis robotic arm as the motion controller to establish the robotic system. The robot's control system was constructed using computer software packages Grasshopper and RoboDK. The storage-extrusion system was independently designed and manufactured as a standalone system, capable of being interconnected with the robotic system. This system allows for the independent setting of extrusion speeds, enabling synchronization with the robotic motion. This synchronization enhances printing quality, ensuring the shape and structural integrity of the printed components.

## 2.3 EXTRUSION SYSTEM

The 3D printing tool head for mortar used in this study was independently designed and manufactured. It primarily employs a microcontroller to control the compression and extrusion of materials using a helical screw. The internal storage unit of the toolhead can accommodate a sufficient quantity of mortar samples for experimentation. Upon receiving the extrusion command, the microcontroller controls the motor rotation, driving the rotation of the screw. The screw, functioning as a rotary positive displacement pump, conveys the material in the axial direction, allowing the mortar to be continuously extruded from the nozzle, as illustrated in Figure 4.

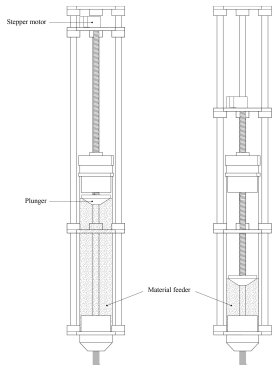


Figure 4. Working principle of the storage-extrusion 3D printing tool head

## 3. Experiment

### 3.1 PROTOTYPING AND GEOMETRY

The Yellow River sand 3D printing mortar holds promising prospects for constructing flood defense walls along river embankments. Considering its potential applications, we have designed a parametric flood defense wall with dimensions of 1000mm in height, 400mm in width, and 120mm in thickness, as depicted in Figure 5.

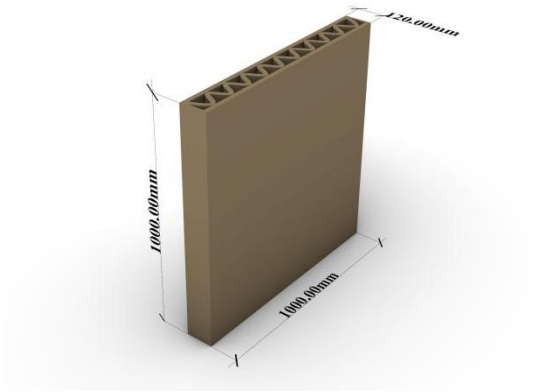


Figure 5. Parametric flood wall designed for 3D printing

A segment of this design was selected as a printed sample for testing, with the sample measuring 100mm in height, 200mm in width, and 120mm in thickness, as shown in Figure 6.

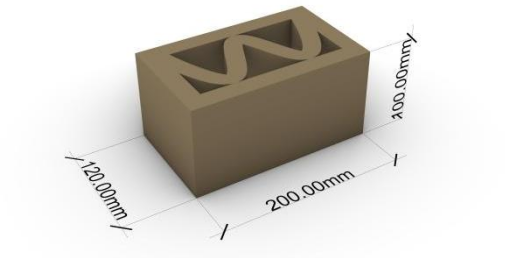


Figure 6. Sample model intended for 3D printing

### 3.2 PARAMETER-BASED CONTROL EXPERIMENT

In the formulation experiments, we conducted preliminary estimations of the printing speed for the mortar sample. After printing multiple linear paths again, we determined the printing speed to be set at 15mm/s. Using Grasshopper, we generated the printing path for this sample segment. The printing path was then analyzed and parsed into the robot's flange workplace using RoboDK, as illustrated in Figure 7.

Subsequently, a robot-readable programming language was generated and transmitted in real-time to the AR4 robot to complete the final 3D printing process.

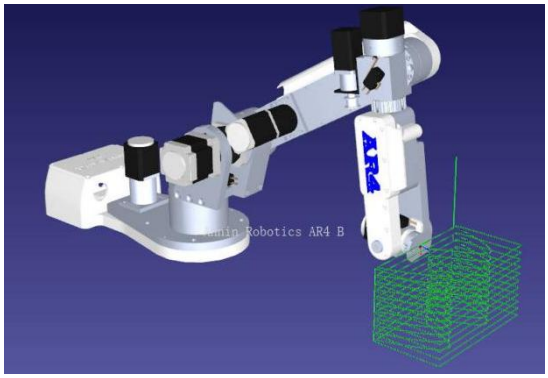


Figure 7. 3D Printing paths generated in RoboDK

## 3.3 EXPERIMENT PROCESS

The final layout of the components and the workbench for the experiment are illustrated in Figure 8. Before commencing the final printing experiment, a dry run was conducted using the robot to ensure the normalcy of the motion along the designated path. Subsequently, the tool head was mounted to check for proper height and assess the risk of potential collisions. After completing these tests, the official commencement of the final printing experiment was initiated. The experiment involved the real-time transmission of programs to the AR4 robot and the extrusion tool head through the RoboDK software and Arduino software within the control system.

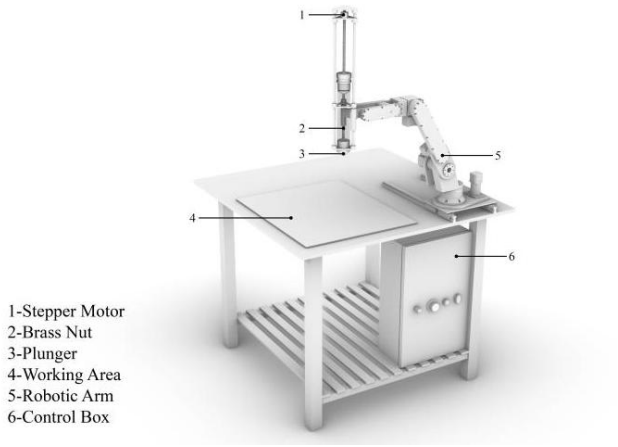


Figure 8. Layout of the final experimental work platform

## 4. Result

The entire experiment concluded in 5 minutes and 18 seconds, successfully producing the sample segment, as depicted in Figure 9.

Figure 9. Images of the final 3D printing process

In this study, we investigated the fundamental parameters of Yellow River sand-based 3D printing mortar and performed printing performance tests on Yellow River sand 3D printing mortar with various ratios. This exploration resulted in the preliminary identification of a formulation suitable for 3D printing of Yellow River sand 3D printing mortar. We established a workflow for Yellow River sand 3D printing by integrating this mortar with a robotic platform and an autonomously developed storage-extrusion system, ultimately achieving the 3D printing of designed samples.

However, due to the tool head employing a mechanical extrusion method and having limited capacity, the extrusion speed of the material could be faster, and the texture could be smoother. Moreover, the material's solidification time is lengthy, and an excessive number of layers may exacerbate the collapse of the first layer. Therefore, this experiment has only completed the 3D printing of two-layer samples.

## 5. Conclusion and Prospect

This study confirms the feasibility and excellent performance of 3D printing mortar using Yellow River sand as fine aggregate. The main conclusions of this research can be summarized in three points.

Firstly, through tests on the printing performance of Yellow River sand 3D printing mortar with various ratios in flowability, setting time, buildability, and extrudability, we have preliminarily identified a formulation suitable for 3D printing with Yellow River sand mortar.

Secondly, by combining a robotic platform with an autonomously developed storage-extrusion 3D printing tool head, practical 3D printing experiments were conducted, validating the flowability, extrudability, and buildability of Yellow River sand 3D printing mortar.

Future research, with continued in-depth exploration of Yellow River sand 3D mortar and 3D printing technology, will further expand the application scenarios for Yellow River sand. This technology and material will garner increased attention, leading to enhanced resource utilization of Yellow River sand. This, in turn, will contribute to reducing sedimentation in the Yellow River, facilitating advancements in construction technology in the Yellow River basin, and playing a crucial role in lowering carbon emissions.

## References

Palacios, J., Paredes, M., Castillo, T., & Paredes, O. (2020). Mortar for 3D printers using River Sand, Portland cement and hydraulic lime. Scientific Review Engineering and Environmental Studies (SREES), 29(4), 399–408. https://doi.org/10.22630/pniks.2020.29.4.34

Zou, S., Xiao, J., Ding, T., Duan, Z., & Zhang, Q. (2021). Printability and advantages of 3D printing mortar with 100% recycled sand. Construction and Building Materials, 273, 121699. https://doi.org/10.1016/j.conbuildmat.2020.121699

Deng, Q., Zou, S., Xi, Y., & Singh, A. (2023). Development and characteristic of 3D-printable mortar with waste glass powder. Buildings, 13(6), 1476. https://doi.org/10.3390/buildings13061476

Gomaa, M., Jabi, W., Veliz Reyes, A., & Soebarto, V. (2021). 3D printing system for Earth-based construction: Case study of cob. Automation in Construction, 124, 103577. https://doi.org/10.1016/j.autcon.2021.103577

Liang, H., Xi, L., Xiao, L., Guo, Li.,& Wenzhan, J. (2020). Research and application of performance based on desert sand 3D printing mortar. Concrete, 374, 108-110. https://doi.org/10.3969/j.issn.1002-3550.2020.12.024

Zhang, Y., Zhang, Y., Liu, G., Yang, Y., Wu, M., & Pang, B. (2018). Fresh properties of a novel 3D printing concrete ink. Construction and Building Materials, 174, 263–271. https://doi.org/10.1016/j.conbuildmat.2018.04.115

Le, T. T., Austin, S. A., Lim, S., Buswell, R. A., Gibb, A. G., & Thorpe, T. (2012). Mix design and fresh properties for high-performance printing concrete. Materials and Structures, 45(8), 1221–1232. https://doi.org/10.1617/s11527-012-9828-z

Ma, G., Li, Z., & Wang, L. (2018). Printable properties of cementitious material containing copper tailings for extrusion based 3D printing. Construction and Building Materials, 162, 613–627. https://doi.org/10.1016/j.conbuildmat.2017.12.051

Le, T. T., Austin, S. A., Lim, S., Buswell, R. A., Law, R., Gibb, A. G. F., & Thorpe, T. (2012). Hardened properties of high-performance printing concrete. Cement and Concrete Research, 42(3), 558–566. https://doi.org/10.1016/j.cemconres.2011.12.003

Marchon, D., Kawashima, S., Bessaies-Bey, H., Mantellato, S., & Ng, S. (2018). Hydration and rheology control of concrete for digital fabrication: Potential admixtures and Cement Chemistry. Cement and Concrete Research, 112, 96–110. https://doi.org/10.1016/j.cemconres.2018.05.014